

# Microdomain model analysis on the negative partial intensity in a disordered ternary alloy

Shinya Hashimoto

Department of Materials Science, Iwaki Meisei University, Iwaki, Fukushima 970-8551, Japan.  
Correspondence e-mail: hashimoto@iwakimu.ac.jp

Received 14 September 1998

Accepted 27 September 1999

Local atomic arrangements expected in a short-range-ordered ternary alloy system are discussed from the theoretical viewpoint of X-ray diffraction by employing a microdomain model, initially developed for a binary alloy system [Hashimoto (1974). *Acta Cryst.* **A30**, 792–798]. It is concluded that a negative partial intensity of short-range-order diffuse scattering is caused by a mixing occupation of two relevant atomic species on the sublattice in the ordered lattice within microdomains, even though there is no heterogeneity of atomic concentration in the alloy crystal, such as a segregation of particular atomic species.

© 2000 International Union of Crystallography  
Printed in Great Britain – all rights reserved

## 1. Introduction

X-ray elastic scattering from a disordered  $A$ – $B$ – $C$  ternary alloy is composed of fundamental reflection and short-range-order (SRO) diffuse scattering. The SRO diffuse scattering can be expressed as a sum of the partial intensities from three kinds of atomic pairs,  $A$ – $B$ ,  $B$ – $C$  and  $C$ – $A$  (Hashimoto *et al.*, 1985; Hashimoto, 1987a):

$$I_{\text{SRO}}(\mathbf{q}) = I_{\text{SRO}}^{AB}(\mathbf{q}) + I_{\text{SRO}}^{BC}(\mathbf{q}) + I_{\text{SRO}}^{CA}(\mathbf{q}), \quad (1)$$

which can be illustrated one-dimensionally as shown in Fig. 1.

The synchrotron-radiation experiment on the  $\text{Cu}_2\text{NiZn}$  alloy by the present author and his co-workers is considered to be one of the successful studies that have separated the X-ray diffuse intensity from a ternary disordered alloy into the partial intensities (Hashimoto *et al.*, 1985). These workers disclosed that the partial intensity from the  $\text{Cu}$ – $\text{Ni}$  pairs appeared as a negative intensity maximum at the 100 and its equivalent superlattice reflection positions. Fig. 1 shows this situation schematically with a negative intensity maximum of  $I_{\text{SRO}}^{BC}$ .

Two theoretical works (Hashimoto, 1987a,b) followed the experiments. One of them (Hashimoto, 1987a) proved mathematically the existence of a negative partial intensity and derived inequality relations among the three partial diffuse intensities. The other (Hashimoto, 1987b) presented a thermodynamical discussion on a ternary alloy system based on the de Fontaine method (de Fontaine, 1972, 1973) in order to characterize the negative partial intensity maximum.

We are now interested in studying the local atomic configuration causing the negative partial intensity. This will be developed by extending the microdomain model that was applied to a SRO binary alloy by the present author (Hashimoto, 1974, hereinafter referred to as paper I). The structure is illustrated schematically in Fig. 2, in which the shaded area

represents a random matrix and the circles represent minute ordered regions or the so-called microdomains. The ordered structure is composed of several sublattices occupied by different atomic fractions. It has been suggested that such a microdomain structure exists in SRO alloys (Gehlen & Cohen, 1965; Greenholz & Kidron, 1970).

## 2. Intensity expression in the microdomain model of a ternary alloy structure

Symbols used in the present paper are listed in Table 1.

The basic equation of the SRO diffuse intensity from a multicomponent alloy, if it has centrosymmetry of interatomic correlation, is expressed as (Hashimoto, 1987a)

$$I_{\text{SRO}}(\mathbf{q}) = - \sum_i \sum_{j(>i)} |f_i - f_j|^2 \sum_m \sum_n \langle \eta_m^i \eta_n^j \rangle \times \exp[-2\pi i \mathbf{q} \cdot (\mathbf{R}_m - \mathbf{R}_n)], \quad (2)$$

where  $f_i$  is the atomic scattering factor of the  $i$ th kind of atom and  $\mathbf{q}$  is the scattering vector. Here, both the static and the dynamic displacements of atoms have been ignored for the sake of brevity.  $\eta_m^i$  is the parameter to represent a concentration deviation from the alloy fraction  $x_i$ , *i.e.*

$$\eta_m^i = \begin{cases} 1 - x_i & \text{if atom of type } i \text{ is at the } m\text{th} \\ & \text{lattice site } \mathbf{R}_m \\ -x_i & \text{otherwise,} \end{cases} \quad (3)$$

which is generally called the Flinn operator (de Fontaine, 1979; Taggart, 1973).

We will develop the SRO intensity equation according to the concept of microdomains as illustrated in Fig. 2. Let the microdomains be labelled with  $1, 2, \dots, u, \dots, N_d$ . We here define a shape function  $E_u(\mathbf{R}_m)$  for the  $u$ th domain:

$$E_u(\mathbf{R}_m) = \begin{cases} 1 & \text{if } \mathbf{R}_m \text{ lies in a domain } u \\ 0 & \text{outside the domain } u. \end{cases} \quad (4)$$

According to paper I, the diffuse-intensity equation (2) can be developed as

$$I_{\text{SRO}}(\mathbf{q}) = I_{\text{RM}}(\mathbf{q}) + I_{\text{MD}}(\mathbf{q}), \quad (5a)$$

where

$$I_{\text{RM}}(\mathbf{q}) = n_r \sum_i \sum_{j(>i)} x_i x_j |f_i - f_j|^2 \quad (5b)$$

and

$$I_{\text{MD}}(\mathbf{q}) = - \sum_i \sum_{j(>i)} |f_i - f_j|^2 \sum_u \sum_m \sum_n \langle \eta_m^i \eta_n^j \rangle \times E_u(\mathbf{R}_m) E_u(\mathbf{R}_n) \exp[-2\pi i \mathbf{q} \cdot (\mathbf{R}_m - \mathbf{R}_n)]. \quad (5c)$$

$n_r$  is the number of atoms in the random matrix,  $I_{\text{RM}}(\mathbf{q})$  reveals the Laue monotonic scattering exclusively from the random matrix and  $I_{\text{MD}}(\mathbf{q})$  the intensity maxima arising from the microdomains. The double summation in equations (5b) and (5c) implies a sum only over the atomic pairs between different species.

We first consider the factor  $\langle \eta_m^i \eta_n^j \rangle$  in equation (5c). We consider that the sites  $m$  and  $n$  belong to the sublattices labelled  $M$  and  $N$ , respectively. Then  $\langle \eta_m^i \eta_n^j \rangle$  can be rewritten as

$$\begin{aligned} \langle \eta_m^i \eta_n^j \rangle &= \langle [(\eta_m^i - H_M^i) + H_M^i][(\eta_n^j - H_N^j) + H_N^j] \rangle \\ &= \langle (\eta_m^i - H_M^i)(\eta_n^j - H_N^j) \rangle + \langle H_M^i H_N^j \rangle, \quad \text{for } i \neq j, \end{aligned} \quad (6)$$

where  $H_M^i$  is the average of  $\eta_m^i$  only on the  $M$ th sublattice. This can be calculated in terms of  $x_i^M$ , the atomic fraction of the  $i$ th atom on the  $M$ th sublattice, as

$$H_M^i = x_i^M(1 - x_i) + \sum_{j(\neq i)} x_j^M(-x_i) = x_i^M - x_i, \quad (7)$$

where we used a conservation rule

$$\sum_i x_i^M = 1. \quad (8)$$

The first term on the right-hand side of equation (6) vanishes for  $m \neq n$  under the assumption that there is no short-range order between the mixing atoms in the ordered lattice. Then it can readily be evaluated that

$$\langle (\eta_m^i - H_M^i)(\eta_n^j - H_N^j) \rangle = -w_{ij}, \quad (9a)$$

where

$$w_{ij} = (1/N_s) \sum_{M=1}^{N_s} x_i^M x_j^M, \quad (9b)$$

in which  $N_s$  is the number of sublattices.  $w_{ij}$  vanishes when each sublattice is occupied by atoms of a single kind, *i.e.* in the case that  $x_i = 1$  and  $x_j = 0$  ( $j \neq i$ ). This is the case that the ordering of atoms in the microdomains is perfect. Thus,  $w_{ij}$  is thought to represent a degree of mixing of atomic species in the ordered lattice. The  $w_{ij}$  term gives a Laue monotonic scattering uniformly distributed in the  $\mathbf{q}$  space or reciprocal space like  $I_{\text{RM}}(\mathbf{q})$ .

Next we investigate the second term in equation (6). It can be written in the form of a Fourier series as

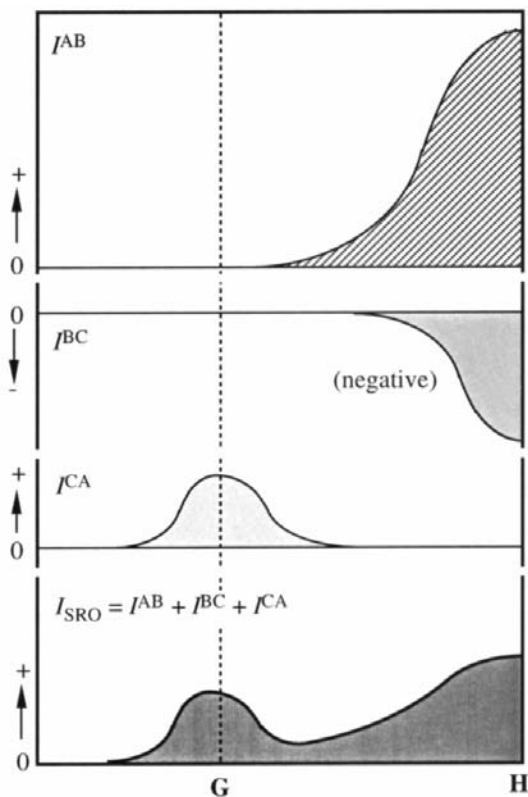


**Figure 1**  
Illustration of the relation between the total and partial short-range-order diffuse scattering intensities. **G** and **H** are some superlattice reflection positions.

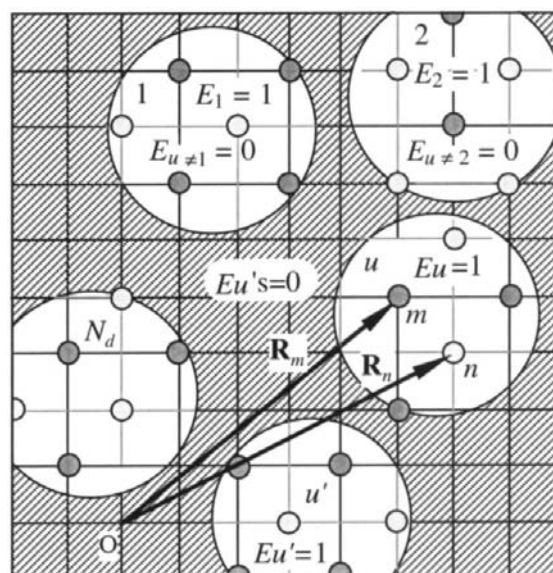


**Figure 2**  
A schematic illustration of a microdomain model for a short-range-ordered alloy. Circles represent the ordered domains and the shaded region the random matrix.

**Table 1**  
Glossary.

$\mathbf{r}$	Positional vector in real space
$\mathbf{R}_m$	Lattice vector for the $m$ th atomic site
$\xi_M$	Step-shift vector of sublattice $M$ with respect to the first sublattice
$\mathbf{q}$	Scattering vector
$\mathbf{G}$	Superlattice reflection position
$i, j$	Labels on the atomic species ( $A, B, C$ )
$m, n$	Labels on the atomic lattice site
$M, J$	Labels on the sublattice in the ordered lattice
$N_s$	The number of sublattices in the ordered lattice
$x_i$	Fraction of $i$ th atomic species
$x_i^M$	Fraction of $i$ th atom on the $M$ th sublattice
$f_i$	Atomic scattering factor of the $i$ th atom
$\eta_m^i$	Flinn's operator of the $i$ th atom for the $m$ th site [defined by equation (3)]
$H_M^i$	Average of $\eta_m^i$ on the $M$ th sublattice of the ordered lattice structure
$n_r$	The number of atoms composing the random matrix
$n_d$	Total number of atoms within all the domains
$n_a$	Total number of atoms in the crystal
$v_0$	Crystal volume per atom
$v_q$	Volume of the Brillouin zone for the fundamental lattice (= $1/v_0$ )
$E_u(\mathbf{R}_m)$	Domain shape function of the $u$ th domain [defined by equation (4)]
$E(\mathbf{r})$	Average shape function of the domains
$\varepsilon(\mathbf{q})$	Fourier transform of the shape function $E(\mathbf{r})$
$w_{ij}$	Mixing parameter of wrong atoms in the ordered lattice of the domain [defined by equation (9b)]
$\zeta_{\mathbf{G}}^{ij}$	Intersublattice correlation parameter [defined by equation (10b)]
$F_{\mathbf{G}}^i$	Partial structure factor of the ordered lattice per atom with respect to atom $i$
$\alpha_i^{ij}$	Warren–Cowley short-range-order parameter [defined by equation (14)]
$\alpha^{ij}(\mathbf{q})$	Fourier transform of the Warren–Cowley parameter $\alpha_i^{ij}$

$$\langle H_M^i H_{M+L}^j \rangle = - \sum_{\mathbf{G}(BZ)} \zeta_{\mathbf{G}}^{ij} \exp(-2\pi i \mathbf{G} \cdot \mathbf{R}_L), \quad (10a)$$

in which

$$\zeta_{\mathbf{G}}^{ij} = -\Re[F_{\mathbf{G}}^i F_{\mathbf{G}}^{j*}], \quad (10b)$$

where

$$F_{\mathbf{G}}^i = (1/N_s) \sum_M H_M^i \exp(2\pi i \mathbf{G} \cdot \xi_M). \quad (10c)$$

$\mathbf{G}$  represents the superlattice reflection position. The summation in equation (10a) is taken over the superlattice reflection positions in the Brillouin zone for the fundamental lattice or the average lattice. The subscript  $M + L$  labels the sublattice translated by an intersublattice vector  $\mathbf{R}_L$  from the sublattice  $M$ .  $\Re[\dots]$  in (10b) implies a real number of  $[\dots]$ , explicitly indicating the centrosymmetry of interatomic correlation (Hashimoto, 1987a).  $\xi_M$  in (10c) is the step-shift vector of the  $M$ th sublattice with respect to the first one. Then  $F_{\mathbf{G}}^i$  is regarded as a sort of structure factor of the ordered structure with respect to the  $i$ th atom. Hereinafter, we call  $F_{\mathbf{G}}^i$  ‘a partial structure factor’.

Now we turn to the factor  $E_u(\mathbf{R}_m)E_u(\mathbf{R}_n)$  in equation (5c). We define a continuous function  $E(\mathbf{r})$  with its centre at  $\mathbf{r} = 0$  as an average shape function of  $E_u(\mathbf{R}_m)$  in real space (see paper I) by

$$\begin{aligned} & (1/N_d) \sum_u \sum_m E_u(\mathbf{R}_m)E_u(\mathbf{R}_{m+l}) \\ & = (1/v_0) \int E(\mathbf{r})E(\mathbf{r} + \mathbf{R}_l) d\mathbf{r}, \end{aligned} \quad (11)$$

where  $N_d$  is the number of domains over the whole crystal and  $v_0$  is the crystal volume per atom. Thus, equation (5c) can be written as

$$I_{\text{MD}}(\mathbf{q}) = \sum_i \sum_{j(>i)} |f_i - f_j|^2 \left[ n_d w_{ij} + N_d \sum_{\mathbf{G}} \zeta_{\mathbf{G}}^{ij} \varepsilon^2(\mathbf{q} - \mathbf{G}) \right], \quad (12a)$$

with

$$\varepsilon(\mathbf{q}) = (1/v_0) \int E(\mathbf{r}) \exp(-2\pi i \mathbf{q} \cdot \mathbf{r}) d\mathbf{r}. \quad (12b)$$

$n_d$  is the total number of atoms involved within all domains. The factor  $\varepsilon^2(\mathbf{q} - \mathbf{G})$  in equation (12a) determines a profile of the diffuse maximum centred at the superlattice reflection position  $\mathbf{G}$ , and also the number of atoms in the single domain by its integration around  $\mathbf{G}$ .  $\zeta_{\mathbf{G}}^{ij}$  determines the sign (positive/negative) of the diffuse maximum at  $\mathbf{G}$  as well as the peak height.

The SRO diffuse intensity per atom can finally be expressed as

$$I_{\text{SRO}}(\mathbf{q})/n_a = \sum_i \sum_{j(>i)} x_i x_j |f_i - f_j|^2 \alpha^{ij}(\mathbf{q}), \quad (13a)$$

where

$$\begin{aligned} \alpha^{ij}(\mathbf{q}) &= (1/n_a) \left[ n_r + (n_d w_{ij}/x_i x_j) \right. \\ & \left. + (N_d/x_i x_j) \sum_{\mathbf{G}} \zeta_{\mathbf{G}}^{ij} \varepsilon^2(\mathbf{q} - \mathbf{G}) \right], \end{aligned} \quad (13b)$$

and  $n_a = n_r + n_d$  is the total number of atoms belonging to the whole alloy crystal. Equation (13b) gives a quantity equivalent to the Fourier transform of  $\alpha_i^{ij}$ , the Warren–Cowley SRO parameter in a multicomponent alloy system, defined as

$$\alpha_i^{ij} = 1 - p_l^{ij}/x_i x_j, \quad (14)$$

where  $p_l^{ij}$  is the *a priori* probability of finding an  $ij$  atomic pair with the interatomic vector  $\mathbf{R}_l$ . The first and second terms on the right-hand side of equation (13b) jointly make a uniform background, which must take a positive value less than unity in Laue units. This ‘unity’ means that all  $i$  and  $j$  atoms are arranged at complete random over the crystal. Some ordering of atoms modifies the background so as to cause positive or negative diffuse maximum at  $\mathbf{G}$ .

### 3. Signs (+/–) of the partial intensities in the model

#### 3.1. Possibility of a negative partial intensity maximum

A negative intensity maximum could be caused if  $\zeta_{\mathbf{G}}^{ij}$  is negative in equation (13b).  $-\zeta_{\mathbf{G}}^{ij}$  defined in equation (10b) gives a scalar product of the vectors  $F_{\mathbf{G}}^i$  and  $F_{\mathbf{G}}^j$  in complex space. The  $F_{\mathbf{G}}^i$ 's make a closed loop, for example, a triangle in a ternary alloy as shown in Fig. 3, since we have a sum rule

$$\sum_i F_{\mathbf{G}}^i = 0, \quad (15)$$

which is derived from equations (7) and (10c). Fig. 3 shows a case of an obtuse-angled triangle; then  $\zeta_{\mathbf{G}}^{BC}$  is negative and the other two,  $\zeta_{\mathbf{G}}^{CA}$  and  $\zeta_{\mathbf{G}}^{AB}$  are positive. If the triangle is acute-angled, all  $\zeta_{\mathbf{G}}^{ij}$  are positive. A right-angled triangle represents the case that one of the  $\zeta_{\mathbf{G}}^{ij}$  is zero.

### 3.2. Consideration of the orientational variants of an ordered lattice

It is known, especially in ordered alloys, that the symmetry of local structure or domain can be lower than that of the averaged structure over the whole alloy. Accordingly, there may exist some orientational variants of the ordered lattice in the present model. This situation is demonstrated in Fig. 4, which shows, as an example, three orientational variants of the CuAu-type ( $L1_0$ ) ordered lattice. The total intensity from the domains with different variants can be written as

$$I_{\text{MD}}(\mathbf{q}) = \sum_i \sum_{j(>i)} |f_i - f_j|^2 \sum_v \left[ n_d w_{ij} + N_d \sum_{\mathbf{G}} \zeta_{\mathbf{G}}^{ij} e^{2i(\mathbf{q} - \mathbf{G})} \right]_v, \quad (16)$$

where  $[\dots]_v$  represents the quantity for the  $v$ th variants of the ordered lattice. For example,  $[n_d]_v$  stands for the total number of atoms belonging to the domains of the  $v$ th variant.  $\sum_v$  indicates the summation over all the variants. Thus, the sign of the partial intensity maximum at  $\mathbf{G}$  is characterized with  $\zeta_{\text{ave}}^{ij}$  defined by

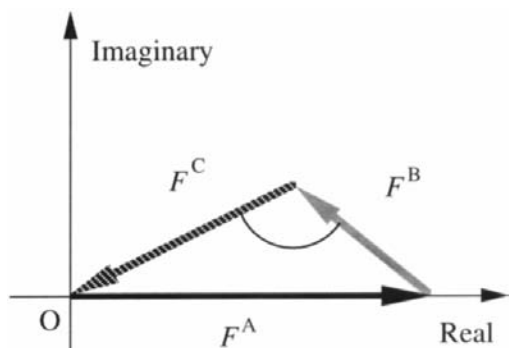


**Figure 3**  
Illustration of three  $F_{\mathbf{G}}^i$  vectors ( $i = A, B$  and  $C$ ) making a closed loop in complex space.

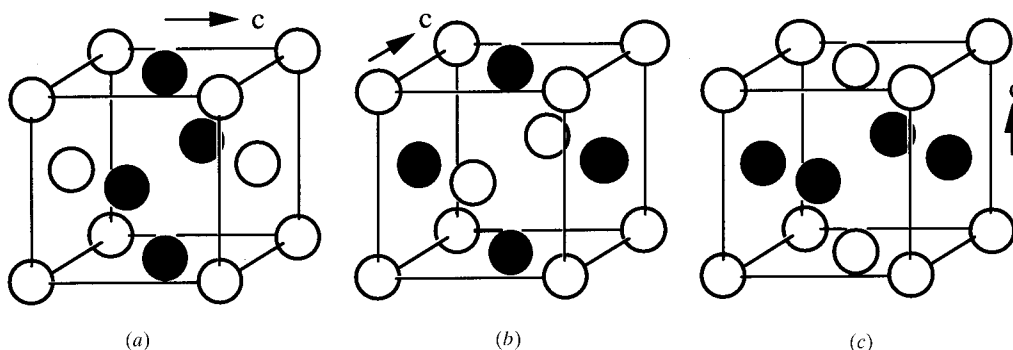


**Figure 4**  
Example of the orientational variants of the ordered lattice, showing three kinds of orientational variants of the  $L1_0$ -type ordered lattice.

$$N_d \zeta_{\text{ave}}^{ij} \equiv \sum_v [N_d \zeta_{\mathbf{G}}^{ij}]_v. \quad (17)$$

### 3.3. Case of the ordered domain structure based on the Cu-type face-centred cubic lattice

**3.3.1. General properties.** We here confine our discussion to the ordered lattices based on the Cu-type face-centred cubic (f.c.c.) structure in which four simple cubic sublattices are distinguished as illustrated in Fig. 5.  $F_{\mathbf{G}}^i$  given in equation (10c) is explicitly expressed as

$$4F_{G_1, G_2, G_3}^i = H_I^i + H_{II}^i \exp[-\pi i(G_1 + G_2)] + H_{III}^i \exp[-\pi i(G_2 + G_3)] + H_{IV}^i \exp[-\pi i(G_3 + G_1)], \quad (18)$$

where  $\mathbf{G} = G_1 \mathbf{b}_1 + G_2 \mathbf{b}_2 + G_3 \mathbf{b}_3$  ( $\mathbf{b}_i$  are the reciprocal-lattice vectors). Equation (18) takes a real number at the superlattice reflection positions (e.g. 100, 010 and 001 in the first Brillouin zone), since  $G_1, G_2$  and  $G_3$  are integers. Thus,  $F_{\mathbf{G}}^i$  ( $i = A, B, C$ ) can be drawn as vectors lying on the real axis, as shown in Fig. 6, which is a special case of Fig. 3.  $\zeta_{\mathbf{G}}^{BC}$  is negative and the others for  $AB$  and  $CA$  are positive, indicating that any one of the  $\zeta_{\mathbf{G}}^{ij}$  must generally be negative.

We next consider the case that the microdomains have different orientational variants of the ordered lattice. If the orientational variants are equally probable, the summation over  $v$  in equation (17) can be replaced by that over  $\mathbf{G}$  in the case of the Cu-type f.c.c. alloy crystal (i.e. over the 100, 010 and 001 reflection positions), and we have

$$\zeta_{\text{ave}}^{ij} \equiv \frac{1}{3} \sum_{\mathbf{G}} \zeta_{\mathbf{G}}^{ij}. \quad (19)$$

This is easily evaluated by putting  $L = 0$  in equation (10a), i.e.

$$\begin{aligned} \zeta_{\text{ave}}^{ij} &= -\frac{1}{12} \sum_{M=1}^4 (x_i^M - x_i)(x_j^M - x_j) \\ &= \frac{1}{3} \left[ x_i x_j - \frac{1}{4} \sum_M x_i^M x_j^M \right]. \end{aligned} \quad (20)$$

Thus, a negative intensity maximum will appear, if the following inequality is realized:

$$x_i x_j < \frac{1}{4} \sum_M x_i^M x_j^M, \quad (21)$$

where the right-hand side is equal to  $w_{ij}$  defined in equation (9b), which arises from the randomness in the ordered domains. The left-hand side of equation (21) represents the Laue monotonic scattering per lattice site for the  $i$  and  $j$  atomic species in the completely disordered state of the alloy. Thus, we cannot expect a negative partial intensity, unless the mixing occupation exists in the sublattices of ordered lattice within the domains. In other words, a condition of  $x_i^M = 1$ , which

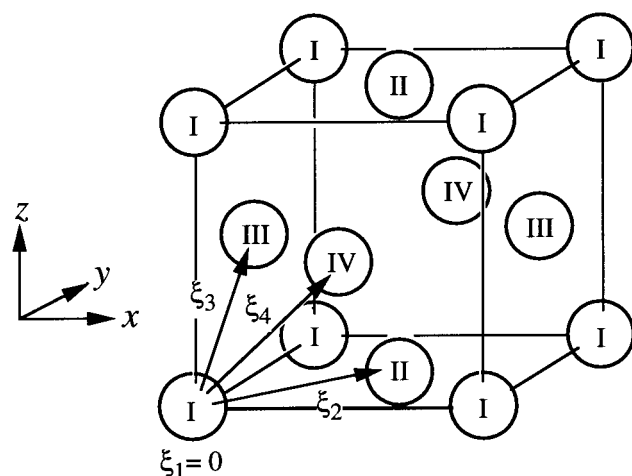


**Figure 5**  
Unit cell of the ordered lattice based on the Cu-type face-centred cubic (f.c.c.) lattice. This is composed of four sublattices.  $\xi_1$ ,  $\xi_2$ ,  $\xi_3$  and  $\xi_4$  are vectors between the sublattice.

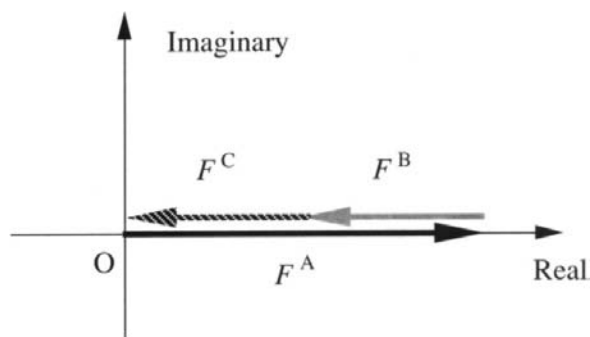


**Figure 6**  
Relation among  $F_G^i$  for the ordered lattice. All the  $F_G^i$  can be real values lying on the real axis by properly choosing the origin in the ordered lattice.

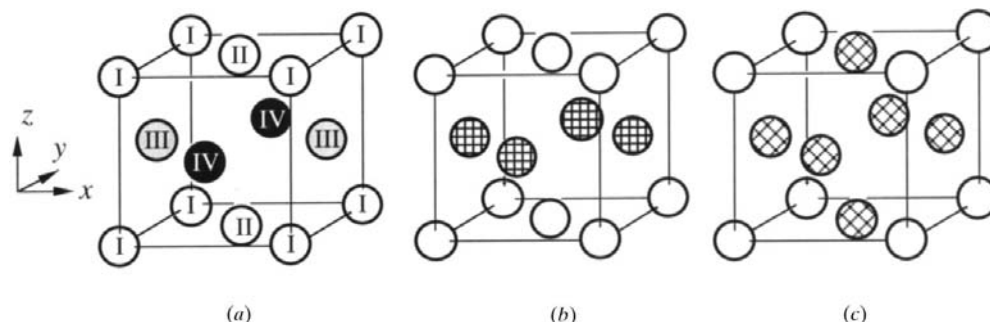


**Figure 7**  
Unit structures for (a) the extended  $L1_0$ , (b) the  $L1_0$  and (c) the  $L1_2$  ordered lattices.

necessarily makes  $x_j^M = 0$  ( $j \neq i$ ), never satisfies equation (21), causing positive maxima for the  $ij$  pairs.

**3.3.2. Application to an  $A_2BC$  alloy.** We will calculate  $\zeta_G^{ij}$  and  $\zeta_{\text{ave}}^{ij}$  for three example structures of the ordered lattice for an  $A_2BC$  ternary alloy, *i.e.* the extended  $L1_0$ ,  $L1_0$  and  $L1_2$  structures.

(a) *Extended  $L1_0$  structure.* We demonstrate a case such that each sublattice can be fully occupied by atoms of a single kind. An  $A_2BC$  alloy enables a perfectly ordered structure in which three kinds of atoms can ideally be assigned to the four sublattices, as shown in Fig. 7(a). This is called the extended  $L1_0$ -type ordered lattice.

Since  $x_i^I = x_i^{II} = \frac{1}{2}(4x_i - x_i^{III} - x_i^{IV})$ , we can evaluate  $\zeta_G^{ij}$  as

$$\zeta_{100}^{ij} = \zeta_{010}^{ij} = -(1/16)(x_i^{III} - x_i^{IV})(x_j^{III} - x_j^{IV}) \quad (22a)$$

and

$$\zeta_{001}^{ij} = -[(x_i^{III} + x_i^{IV})/2 - x_i][(x_j^{III} + x_j^{IV})/2 - x_j], \quad (22b)$$

by using equation (18).

As the first example, putting  $x_A^I = x_A^{II} = x_A^{III} = x_A^{IV} = 1$  and the other fractions  $x_i^M = 0$ , we can have  $\zeta_G^{ij}$  values as listed in the column headed '1' in Table 2, indicating that the partial intensity for a  $B-C$  atomic pair has a negative maximum at the 001 superlattice reflection position.

As already mentioned, the partial intensity belonging to each superlattice reflection position is experimentally observed as an average of the contributions from the three different orientational variants. The average values are also listed in the same column of Table 2, indicating that all of them are positive. This does not contradict the inequality condition (21) for a negative value. That is, the observable partial intensities are all positive in the case that the extended  $L1_0$  lattice structure is perfectly (or ideally) ordered in the domains.

(b)  *$L1_0$  structure.* The column headed '2' in Table 2 gives the extreme case of atom mixing in the extended  $L1_0$  structure, *i.e.*  $x_B^{III} = x_B^{IV}$  and  $x_C^{III} = x_C^{IV}$ . This corresponds to the  $L1_0$  type as illustrated in Fig. 7(b). We can see that  $\zeta_{001}^{BC}$  is negative and the others are positive at the 001 position, and that  $\zeta_G^{ij}$  vanish at the 100 and 010 positions.  $\zeta_{\text{ave}}^{BC}$  is negative at all of the 100, 010 and 001 superlattice reflection positions, indicating that the atom mixing causes the negative intensity maximum related to equation (21).

(c)  $L1_2$  structure. Here we turn to the  $L1_2$ -type ordered lattice (Fig. 7c). Three sublattices (II, III and IV) are occupied by atomic species with the same fractions, *i.e.*  $x_i^{\text{II}} = x_i^{\text{III}} = x_i^{\text{IV}}$  ( $i = A, B, C$ ). Thus,  $\zeta_G^{ij}$  is calculated as

$$\begin{aligned} \zeta_{100}^{ij} = \zeta_{010}^{ij} = \zeta_{001}^{ij} &= -\frac{1}{16}(x_i^{\text{I}} - x_i^{\text{II}})(x_j^{\text{I}} - x_j^{\text{II}}) \\ &= -\frac{1}{9}(x_i^{\text{I}} - x_i)(x_j^{\text{I}} - x_j). \end{aligned} \quad (23)$$

The columns 3, 4 and 5 in Table 2 list example values of  $\zeta_{100}^{ij}$  for three typical cases, illustrated in Figs. 8(a), 8(b) and 8(c), respectively. Column 3 is given for a case that *B* atoms fully occupy the sublattice I and the other kinds of atoms randomly occupy the II, III and IV sublattices with fractional occupancy probabilities. This random mixture of *C* and *A* atoms causes a negative  $\zeta_{100}^{CA}$  by satisfying the inequality relation (21). This negativity of intensity for the *C*–*A* pair at the 100, 010 and 001 superlattice reflection positions must be compensated with the uniform background intensity due to  $w_{CA}$ .

The case of column 4, in which the sublattice I is mainly occupied by *A* atoms, is quite different, but this atomic arrangement gives almost the same ratio and signs among the maxima as in the case of column 3, but causes much smaller magnitudes.

In the case of column 5, in which *A* atoms are distributed all over the sublattices without any preference, *i.e.*  $F_G^A = 0$ , we can see that no partial intensity maxima appear for the pairs including *A* atoms, *i.e.* *AB* and *CA*.

#### 4. Conclusions

In the present work, the X-ray intensity from the short-range order (SRO) in a ternary alloy has been discussed under the assumption that the alloy is constructed with minute ordered regions or microdomains and a random matrix surrounding the domains. The X-ray diffuse intensity scattered from this alloy model is expressed as a sum of three terms, *i.e.* the Laue monotonic scattering from the random matrix, the monotonic scattering due to the atom mixing in the ordered lattice within the domains, and the diffuse maxima due to the ordering in the domains.

**Table 2**

Example calculation of  $\zeta_G^{ij}$  and  $w_{ij}$  values for various internal domain structures of the extended  $L1_0$ ,  $L1_0$  and  $L1_2$  types in an  $A_2BC$  alloy.

Column 1: extended  $L1_0$  type,  $x_A^{\text{I}} = x_A^{\text{II}} = x_B^{\text{III}} = x_C^{\text{IV}} = 1$  and other fractions  $x_i^{\text{M}} = 0$  (Fig. 7a). Column 2:  $L1_0$  type,  $x_B^{\text{II}} = x_B^{\text{IV}}$  and  $x_C^{\text{III}} = x_C^{\text{IV}}$  (Fig. 7b). Columns 3, 4, 5:  $L1_2$  type (Fig. 7c).  $A_2BC$  alloy:  $x_A = 0.5$ ,  $x_B = 0.25$  and  $x_C = 0.25$ .  $\zeta_{\text{ave}}^{ij} = \frac{1}{3}(\zeta_{100}^{ij} + \zeta_{010}^{ij} + \zeta_{001}^{ij})$ .  $\zeta_{010}^{ij} = \zeta_{100}^{ij}$ .

		1	2	3	4	5
$x_i^{\text{I}}$	<i>A</i>	1.0000	1.0000	0.0000	0.6000	0.5000
	<i>B</i>	0.0000	0.0000	1.0000	0.1000	0.5000
	<i>C</i>	0.0000	0.0000	0.0000	0.3000	0.0000
$x_i^{\text{II}}$	<i>A</i>	1.0000	1.0000	0.6667	0.4667	0.5000
	<i>B</i>	0.0000	0.0000	0.0000	0.3000	0.1667
	<i>C</i>	0.0000	0.0000	0.3333	0.2333	0.3333
$x_i^{\text{III}}$	<i>A</i>	0.0000	0.0000	0.6667	0.4667	0.5000
	<i>B</i>	1.0000	0.5000	0.0000	0.3000	0.1667
	<i>C</i>	0.0000	0.5000	0.3333	0.2333	0.3333
$x_i^{\text{IV}}$	<i>A</i>	0.0000	0.0000	0.6667	0.4667	0.5000
	<i>B</i>	0.0000	0.5000	0.0000	0.3000	0.1667
	<i>C</i>	1.0000	0.5000	0.3333	0.2333	0.3333
$\zeta_{100}^{ij}$	<i>BC</i>	0.0625	0.0000	0.0208	0.0008	0.0069
	<i>CA</i>	0.0000	0.0000	−0.0139	−0.0005	0.0000
	<i>AB</i>	0.0000	0.0000	0.0417	0.0017	0.0000
$\zeta_{001}^{ij}$	<i>BC</i>	−0.0625	−0.0625	0.0208	0.0008	0.0069
	<i>CA</i>	0.1250	0.1250	−0.0139	−0.0005	0.0000
	<i>AB</i>	0.1250	0.1250	0.0417	0.0017	0.0000
$\zeta_{\text{ave}}^{ij}$	<i>BC</i>	0.0208	−0.0208	0.0208	0.0008	0.0069
	<i>CA</i>	0.0417	0.0417	−0.0139	−0.0005	0.0000
	<i>AB</i>	0.0417	0.0417	0.0417	0.0017	0.0000
$w_{ij}$	<i>BC</i>	0.0000	0.1250	0.0000	0.0600	0.0417
	<i>CA</i>	0.0000	0.0000	0.1667	0.1267	0.1250
	<i>AB</i>	0.0000	0.0000	0.0000	0.1200	0.1250

On the other hand, the total intensity is experimentally observed to be positive as a superposition of the partial intensities for the *AB*, *BC* and *CA* pairs in an *A*–*B*–*C* ternary alloy. The partial intensities are known to be obtainable separately *via* the anomalous-scattering method by use of several kinds of incident X-rays with different energies (Hashimoto *et al.*, 1985). We found, in the microdomain

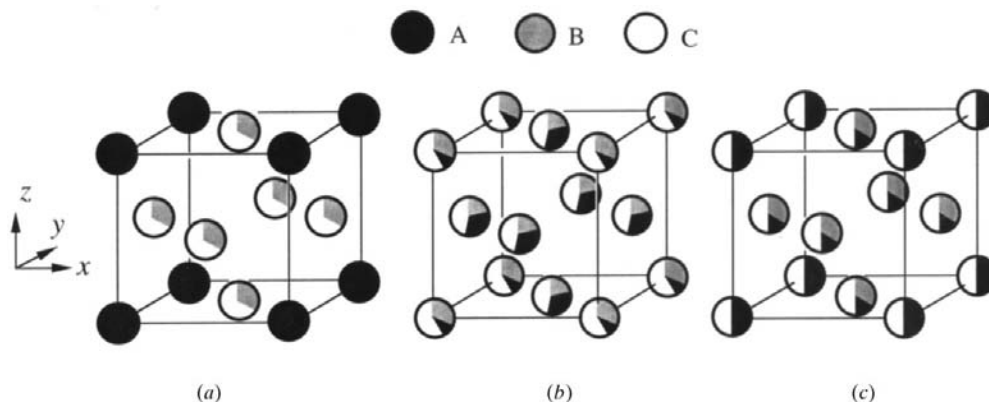


**Figure 8**

Structure models with different atomic fractions for the  $L1_2$ -type ordered lattice taken as examples in the calculation. (a) Structure corresponding to column 3 in Table 2, (b) that corresponding to column 4 and (c) that corresponding to column 5.

structure of SRO, that any one of the three partial intensity maxima for the  $AB$ ,  $BC$  and  $CA$  pairs necessarily takes a negative value at every superlattice reflection position  $\mathbf{G}$  coinciding with the sign of  $\zeta_{\mathbf{G}}^{ij}$  given in equation (10b). In other words, all the partial intensity maxima cannot be positive simultaneously, since  $-\zeta_{\mathbf{G}}^{ij}$  is given as a scalar product between two of the three partial structure factors  $F_{\mathbf{G}}^{ij}$  ( $i = A, B, C$ ), which make a closed loop just on the real axis in complex space (see Fig. 6).

In the case that ordered domains are locally stabilized with a lower rotational symmetry than that of the overall structure of the alloy, the total SRO intensity may be observed as a superposition of the reflections of different indices from the orientational variants of the ordered lattice. If the fundamental (or average) lattice is based on the Cu-type f.c.c. lattice, all the partial intensities can be positive in a special case. It is the inequality relation (21) that determines whether the partial intensity takes a negative maximum or not. The relation shows that all the observed maxima in reciprocal space must be positive, if each variant has a highly ordered structure. Atom mixing or some disordering on the sublattices can satisfy the inequality relation so that any of the partial intensities may be negative.

Thus, we can meet the possibility of observing a negative partial intensity maximum when one of the following conditions is satisfied.

(i) The rotational symmetry of the ordered structure in a domain and that of the overall alloy structure are identical, which generates a microdomain structure with a single orientational variant of order.

(ii) In the case that the locally ordered lattice has a lower rotational symmetry than that of the overall fundamental lattice, which generates several variants of different orientations, the atom mixing on the sublattices is enhanced so as to satisfy the inequality relation (21).

The conditions (i) and (ii) do not contradict each other. The  $L1_2$ -type ordered structure can exist as a single variant in the random matrix, causing negative partial intensity for any one of the pairs. Even the average of the independent reflections gives the same signs. This shows that the  $L1_2$  structure intrinsically includes atom mixing on the sublattices, enough to satisfy the inequality relation (21).

Inversely, we can say that, if we find all the partial intensities to be positive, the SRO state can be interpreted as having highly ordered orientational variants and causing the diffuse maximum as a superposition from the variants.

## References

- Fontaine, D. de (1972). *J. Phys. Chem. Solids*, **33**, 297–310.  
 Fontaine, D. de (1973). *J. Phys. Chem. Solids*, **34**, 1285–1304.  
 Fontaine, D. de (1979). *Solid State Physics*, Vol. 34, edited by H. Ehrenreich, F. Seitz & D. Turnbull, pp. 73–274. New York: Academic Press.  
 Gehlen, P. C. & Cohen, J. B. (1965). *Phys. Rev.* **139**, A844–A855.  
 Greenholz, M. & Kidron, A. (1970). *Acta Cryst.* **A26**, 311–314.  
 Hashimoto, S. (1974). *Acta Cryst.* **A30**, 792–798.  
 Hashimoto, S. (1987a). *Acta Cryst.* **A43**, 481–485.  
 Hashimoto, S. (1987b). *J. Appl. Cryst.* **20**, 182–186.  
 Hashimoto, S., Iwasaki, H., Ohshima, K., Harada, J., Sakata, M. & Terauchi, H. (1985). *J. Phys. Soc. Jpn.* **54**, 3796–3807.  
 Taggart, G. B. (1973). *J. Phys. Chem. Solids*, **34**, 1917–1921.